

## RESEARCH ARTICLE

10.1002/2017JC012741

## Special Section:

Oceanic Responses and  
Feedbacks to Tropical  
Cyclones

## Key Points:

- Preexisting extremely warm SST well absorbs the strong cooling effect and contributes to large air-sea flux for Patricia's intensification
- EP, CP El Niño buildup, and EP decaying year can provide well conditions for hurricane intensification especially along the Americas' coast
- 2015 is the strongest El Niño ever observed. The special warm oceanic feature in October 2015 contributes to Patricia's extraordinary growth

## Supporting Information:

- Supporting Information S1

## Correspondence to:

I.-I. Lin,  
iilin@as.ntu.edu.tw

## Citation:

Huang, H.-C., J. Boucharel, I.-I. Lin, F.-F. Jin, C.-C. Lien, and I.-F. Pun (2017), Air-sea fluxes for Hurricane Patricia (2015): Comparison with supertyphoon Haiyan (2013) and under different ENSO conditions, *J. Geophys. Res. Oceans*, 122, doi:10.1002/2017JC012741.

Received 31 JAN 2017

Accepted 22 MAY 2017

Accepted article online 26 MAY 2017

## Air-sea fluxes for Hurricane Patricia (2015): Comparison with supertyphoon Haiyan (2013) and under different ENSO conditions

Hsiao-Ching Huang<sup>1</sup> , Julien Boucharel<sup>2</sup> , I.-I. Lin<sup>1</sup> , Fei-Fei Jin<sup>2,3</sup> , Chun-Chi Lien<sup>1</sup> , and  
Iam-Fei Pun<sup>1</sup> 

<sup>1</sup>Department of Atmospheric Sciences, National Taiwan University, Taipei, Taiwan, <sup>2</sup>Department of Atmospheric Sciences, SOEST, University of Hawaii at Manoa, Honolulu, Hawaii, <sup>3</sup>Laboratory for Climate Studies, Beijing Climate Center, Chinese Meteorological Agency, Beijing, China

**Abstract** Hurricane Patricia formed on 20 October 2015 in the Eastern Pacific and, in less than 3 days, rapidly intensified from a Tropical Storm to a record-breaking hurricane with maximum sustained winds measured around 185 knots. It is almost 15 knots higher than 2013's supertyphoon Haiyan (the previous strongest tropical cyclone (TC) ever observed). This research focuses on analyzing the air-sea enthalpy flux conditions that contributed to Hurricane Patricia's rapid intensification, and comparing them to supertyphoon Haiyan's. Despite a stronger cooling effect, a higher enthalpy flux supply is found during Patricia, in particular due to warmer pre-TC sea surface temperature conditions. This resulted in larger temperature and humidity differences at the air-sea interface, contributing to larger air-sea enthalpy heat fluxes available for Patricia's growth (24% more than for Haiyan). In addition, air-sea fluxes simulations were performed for Hurricane Patricia under different climate conditions to assess specifically the impact of local and large-scale conditions on storm intensification associated with six different phases and types of El Niño Southern Oscillation (ENSO) and long-term climatological summer condition. We found that the Eastern Pacific El Niño developing and decaying summers, and the Central Pacific El Niño developing summer are the three most favorable ENSO conditions for storm intensification. This still represents a 37% smaller flux supply than in October 2015, suggesting that Patricia extraordinary growth is not achievable under any of these typical ENSO conditions but rather the result of the exceptional environmental conditions associated with the buildup of the strongest El Niño ever recorded.

## 1. Introduction

The Eastern Pacific Ocean is the second most active basin on earth for tropical cyclone (TC) activity but has not quite grabbed fully the attention of the hurricane research community, essentially because most TCs intensify westward, far from inhabited coastlines therefore rarely making any landfalls. However, some systems can recline toward the west coast of North America and potentially impact drastically the U.S. and Mexico [Jauregui, 2003; Ritchie et al., 2011; Raga et al., 2013; Wood and Ritchie, 2013]. As such, Hurricane Patricia formed as a Tropical Depression on 20 October 2015 around (94.0°W, 13.4°N), developed into a Tropical Storm on 21 October, and then after reaching Category 1 (according to the Saffir-Simpson scale) on 22 October, rapidly increased to 185 knots, a record-breaking intensity well exceeding the Category 5 threshold of 135 knots in only 30 hours [Foltz and Balaguru, 2016; Kimberlain et al., 2016; Fu et al., 2017; Rogers et al., 2017]. Its maximum intensity even surpassed 2013 supertyphoon Haiyan (170 knots) [Lin et al., 2014; Lander et al., 2014; Takagi et al., 2016] and Patricia became the strongest hurricane in recorded history. Patricia finally reached Mexico's coastline and rapidly weakened to a Category 2 hurricane on 24 October. Even if Patricia did not caused the fierce damages as for example Iniki in Hawaii in 1992 [Chu and Wang, 1997], it has definitely put the Eastern Pacific TC basin back on the map for both the scientific community and the public.

Tropical cyclone's intensification processes are related to the storm structure, and the surrounding ocean and atmospheric environmental conditions [Gray, 1979; DeMaria, 1996; Emanuel, 1999; Frank and Ritchie, 1999, 2001; Shay et al., 2000; Kaplan and DeMaria, 2003; Goni and Trinanes, 2003; Emanuel et al., 2004; Lin

*et al.*, 2005; Goni *et al.*, 2009; Murakami *et al.*, 2013; Lin and Chan, 2015]. Via air-sea enthalpy fluxes, the ocean provides an important energy source for TC's strengthening [Emanuel, 1986, 1999; Shay *et al.*, 2000; Black *et al.*, 2007; Lin *et al.*, 2008, 2009a, 2013a, 2013b]. Because TCs interact with the entire upper ocean [Price, 1981, 2009], not only sea surface temperature (SST) but also subsurface ocean conditions (generally from surface down to 100 m depth) are critical to assess TCs theoretical maximum intensity [Lin *et al.*, 2008, 2013b; Mainelli *et al.*, 2008; Pun *et al.*, 2011, 2013]. As TCs pass over the ocean, intense winds cause entrainment mixing and upwelling to bring up the deep cold water and cool the SST [Chang and Anthes, 1978; Price, 1981]. This is an unfavorable mechanism to TC intensification, known as the SST cooling effect [Emanuel, 1999; Bender and Ginis, 2000; Lin *et al.*, 2009b; Yablonski and Ginis, 2008; Mei *et al.*, 2015; Wu *et al.*, 2016].

Recently, Jin *et al.* [2014] showed that the meridional discharge [Jin, 1997] of equatorial subsurface heat toward the Eastern Pacific TC region following an El Niño event could lead to a significantly more active hurricane season. While this mechanism of "storm fueling" through redistribution of subsurface heat operates during the TC season that follows the boreal wintertime peak of El Niño, one can wonder how El Niño buildup can affect surface and subsurface conditions and ultimately the processes of TC intensification [Zheng *et al.*, 2015]. In particular, Hurricane Patricia developed in October 2015, a few months before the record-breaking peak of the 2015 El Niño episode, but the subsurface conditions in the region of TC influence, especially along the coast of Central America, were already exceptionally warm, once again reminding us that every El Niño event may not be quite the same [Johnson, 2013; Bond *et al.*, 2015].

In this study, we explore the air-sea enthalpy flux conditions during the intensification of Hurricane Patricia and compare them to supertyphoon Haiyan's (2013). Hurricane Patricia and supertyphoon Haiyan are the 2 "Champion" Tropical Cyclones in the recorded human history. Their maximum intensity were much higher than most of the existing category 5 supertyphoons, i.e. *Katrina* (2005), *Celia* (2010), and *Megi* (2010) peaked at ~140–160 knots [Scharroo *et al.*, 2005; Goni *et al.*, 2011]. These 2 cyclones can be called "category 6 [Lin *et al.*, 2014]" super cyclones, because both reached an astonishing peak intensity, far exceeding the existing highest category of "5" in the Saffir-Simpson Tropical Cyclone Scale. (As suggested by Lin *et al.* [2014], in the Saffir-Simpson Tropical Cyclone Scale, the gap between the minimum threshold values for each consecutive category is about 13–22 knots and the category 5 threshold is 135 knots. Therefore, even if adding another 22–25 knots above category 5 threshold to form a new "category 6" with a threshold value of 160 knots, Patricia and Haiyan are still 25 and 10 knots higher than the "category 6" threshold. Not only intensity, it is also worthwhile to consider the concept of the Accumulated Cyclone Energy (ACE, sum of the square of maximum wind speed over a cyclone's lifetime [Bell *et al.*, 2000; Camargo and Sobel, 2005]). If using the maximum wind speed to estimate cyclone's kinetic energy at peak to a first order, the corresponding square of maximum wind speed of a "category 6" (160–185 knots) TC would be 131–175% higher than a "category 5" TC of 140 knots.) It is intriguing to compare the situation for these two "Category 6" TCs [Lin *et al.*, 2014; Lander *et al.*, 2014; Comiso *et al.*, 2015; Shu *et al.*, 2015; Wada, 2015; Foltz and Balaguru, 2016; Kimberlain *et al.*, 2016; Nakamura *et al.*, 2016; Takagi *et al.*, 2016; Fu *et al.*, 2017; Rogers *et al.*, 2017] over the two sides of the Pacific basin, i.e. Hurricane Patricia to the Mexico versus supertyphoon Haiyan to the Phillipines. We also assess and compare the air-sea flux conditions, if Patricia was "born" under different climate conditions associated with different phases or types of El Niño Southern Oscillation (ENSO). Different modes of ENSO expression are characterized by different large-scale environmental conditions and therefore have a contrasted influence on the seasonal TC activity in the Eastern Pacific [Boucharel *et al.*, 2016a]. Here we focus in particular on the two main ENSO modes and their potential influence on TC intensification, i.e., the so-called Eastern Pacific (EP) and Central Pacific (CP) El Niño [Kug *et al.*, 2009; Yeh *et al.*, 2009] and both their buildup and decaying phases.

The rest of the paper is organized as follows. Data and methods are described in section 2. The third section is dedicated to the comparison between Patricia and Haiyan. In the fourth section, similarly to the recent paper by Boucharel *et al.* [2016a], we compare the 2015 El Niño conditions under which Patricia formed and intensified to the typical conditions found during different flavors and phases of ENSO, and also more specifically to those associated with the two previous strongest EP El Niño events on record, 1982 and 1997. Finally, section 5 provides a discussion of our main results followed by concluding remarks.

## 2. Data and Methods

Hurricane Patricia and supertyphoon Haiyan's data (trajectories and intensity) are obtained from the best track archives of National Hurricane Center's (NHC; <http://ftp.nhc.noaa.gov/atcf/archive/>) and the US Joint

Typhoon Warning Centre (JTWC; [https://metoc.ndbc.noaa.gov/web/guest/jtwc/best\\_tracks/](https://metoc.ndbc.noaa.gov/web/guest/jtwc/best_tracks/)), respectively. The ocean temperature data are obtained from the operational data sets produced routinely by the Global Ocean Data Assimilation System (GODAS) of National Oceanic and Atmospheric Administration (NOAA), National Centers for Environmental Prediction (NCEP). For modeling input and validation of the reanalysis data, we also use the ocean in situ depth-temperature profiles from the “Array for Real-time Geostrophic Oceanography” (Argo) floats near Patricia’s track to obtain the depth of the 26°C and 20°C isotherms (D26 and D20), and finally derive tropical cyclone heat potential (TCHP, i.e., the integrated heat content from SST down to D26) [Shay et al., 2000; Pun et al., 2007, 2014; Mainelli et al., 2008].

To study the response of the upper ocean to the passage of a hurricane (or tropical cyclone (TC)), the response within the upper ocean and SST are emphasized. Here we use the three-dimensional Price-Weller-Pinkel (3DPWP) ocean mixed layer model [Price, 1981; Price et al., 1986, 1994] (supporting information Text S1) to obtain the SST cooling effect (averaged over an area equivalent to 2.5 times the radius of maximum wind) [Huang et al., 2015]. After quantifying the cooling effects from the 3DPWP simulations, we calculate enthalpy fluxes (sensible and latent heat fluxes (SHF and LHF)) based on the bulk aerodynamic formula under TC-ocean coupling condition [Black et al., 2007; Cione et al., 2013; Lin et al., 2014] as follows:

$$\text{SHF } Q_S = C_H W (T_s - T_a) \rho_a C_{pa}$$

$$\text{LHF } Q_L = C_E W (q_s - q_a) \rho_a L_{va}$$

where  $C_H$  and  $C_E$  are the sensible and latent heat exchange coefficients,  $W$  is ocean surface wind speed,  $T_s$  and  $T_a$  are during-TC SST ( $SST_{\text{mixed}} = SST_{\text{preTC}} - \text{SST cooling}$ ) and near-surface air temperature,  $q_s$  and  $q_a$  are surface and air specific humidity, and  $\rho_a$ ,  $C_{pa}$ , and  $L_{va}$  are air density, heat capacity of the air, and latent heat of vaporization.

For the air-sea flux calculation, the near-surface air temperature ( $T_a$ ) and the air specific humidity ( $q_a$ ) were derived from NOAA-NCEP/National Center for Atmospheric Research (NCAR) Reanalysis 1. From the bulk aerodynamic formula, we can see that under higher pre-TC SST ( $SST_{\text{preTC}}$ ), weaker cooling effect, or smaller  $T_a$  and  $q_a$  will contribute to larger air-sea temperature and humidity difference at the TC air-ocean interface, thus allowing more sensible and latent heat flux supply from ocean to support storm intensification.

The vertical wind shear, i.e., the difference in wind between the 200 and 850 hPa atmospheric levels [DeMaria, 1996] is calculated as follows:

$$VWS = \sqrt{(u_{200} - u_{850})^2 + (v_{200} - v_{850})^2}$$

where  $u_{200}$  (resp.  $u_{850}$ ) is the zonal wind component at 200 hPa (resp. 850 hPa) atmospheric level, and  $v_{200}$  (resp.  $v_{850}$ ) is the meridional wind component at 200 hPa (resp. 850 hPa) atmospheric level. We obtain the wind data as well as  $T_a$  and  $q_a$  from the NCEP/NCAR Reanalysis 1.

### 3. Air-Sea Flux Conditions for Supertyphoon Haiyan (2013) and Hurricane Patricia (2015)

Figure 1, supporting information Figure S1, and Figure 2a compare the preexisting ocean conditions for these two record-breaking TCs. Figure 1 and supporting information Figure S1 show monthly data from GODAS reanalysis and Figure 2 from the closest Argo floats’ profiles along Haiyan and Patricia’s trajectories (magenta triangle marks in Figures 1a and 1e, respectively). In both cases, the pre-TC SST is very warm (30.2°C for Patricia and 29.2°C for Haiyan) based on the Argo in situ observations (Table 1). However, subsurface ocean conditions for Patricia are not as favorable as compared to Haiyan’s. As can be seen in Table 1, Figure 1, supporting information Figure S1, and Figure 2a, although deeper than climatological values, pre-Patricia’s D26 and D20 are much shallower (e.g. D26 ~ 70 m) than Haiyan’s (~103 m). Small differences are also found for TCHP, with values around 118 kJ/cm<sup>2</sup> for Haiyan as compared to 104 kJ/cm<sup>2</sup> for Patricia (Table 1).

Figure 2b illustrates the respective TC-induced ocean cooling computed from the 3DPWP model [Price et al., 1994], using the averaged pre-TC Argo profiles as input (Figure 2a). Results suggest the TC-induced ocean cooling effect was smaller for Haiyan than Patricia throughout the intensification process (from TS to peak)

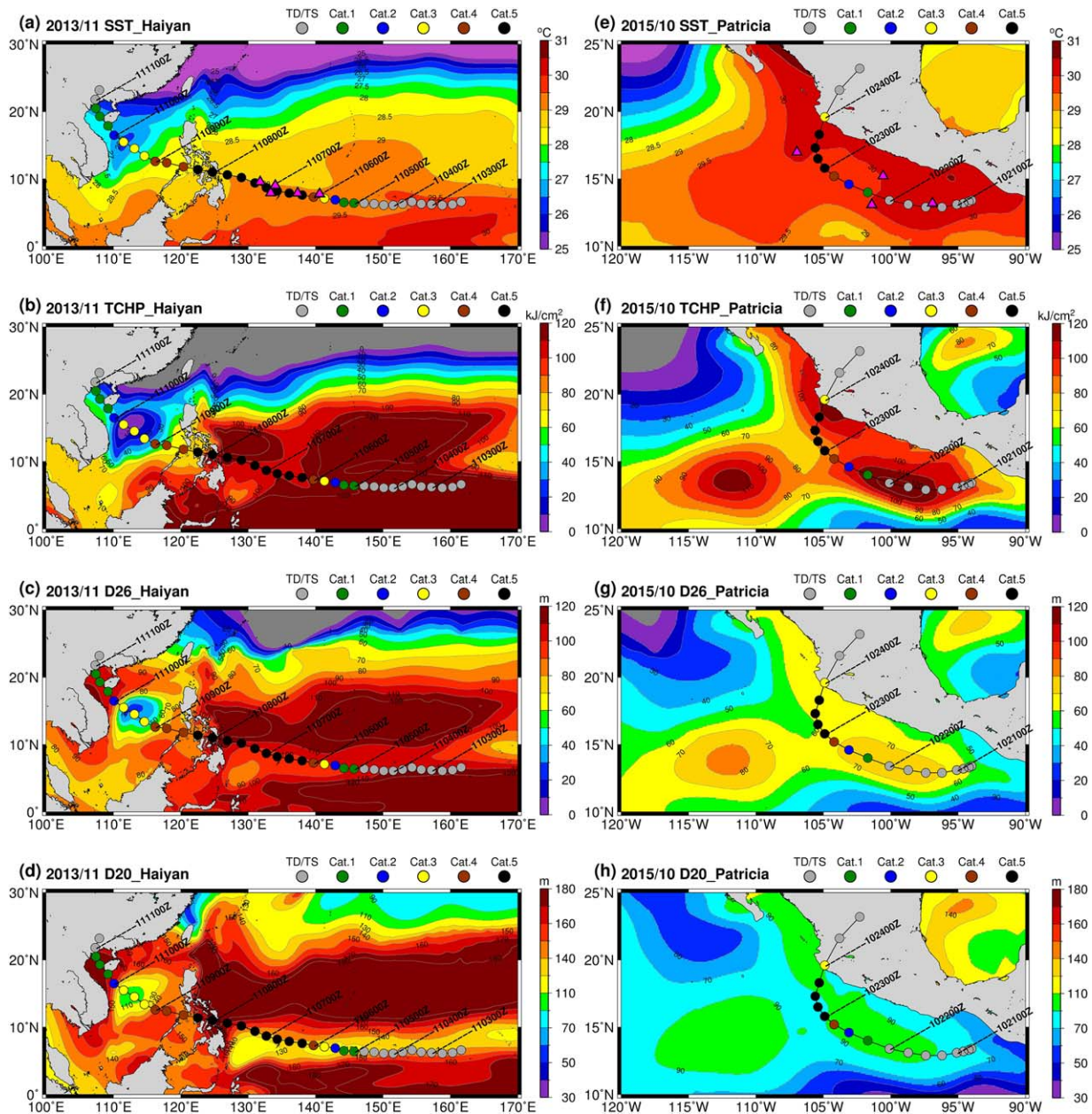


**Figure 1.** (left) Haiyan (November 2013 in the Western North Pacific) and (right) Patricia (October 2015 in the Eastern North Pacific) preexisting ocean conditions are (a) monthly mean sea surface temperature (SST), (b) tropical cyclone heat potential (TCHP), (c) depth of 26°C isotherms (D26), and (d) depth of 20°C isotherms (D20) in November 2013 with trajectories and intensity of Haiyan superimposed. (e–h) The same but in October 2015 for Hurricane Patricia.

(Figure 2c and Table 2a). However, the corresponding air-sea enthalpy (sensible and latent heat) flux supply reverses from the cooling effect. As can be seen in Figure 2c and Table 2a, there was about 24% more enthalpy flux supply for Patricia than Haiyan during their intensification and up to their respective lifetime peak (2218 versus 1788 W/m<sup>2</sup>, respectively). It is consistent with the observed higher intensity of Patricia (185 knots) as compared to Haiyan (170 knots).

This is counterintuitive as a smaller cooling effect usually leads to more enthalpy flux available for storm intensification. This unexpected behavior can be explained by the critical control of the air-sea temperature and humidity differences on the strength of air-sea enthalpy fluxes (see bulk formula in section 2). The during-TC air-sea temperature difference is calculated as  $\Delta T = SST_{mixed} - T_a$ , with  $SST_{mixed} = SST_{preTC} - \text{ocean cooling effect}$ . Therefore, a much warmer  $SST_{preTC}$  for Patricia (30.2°C versus 29.2°C for

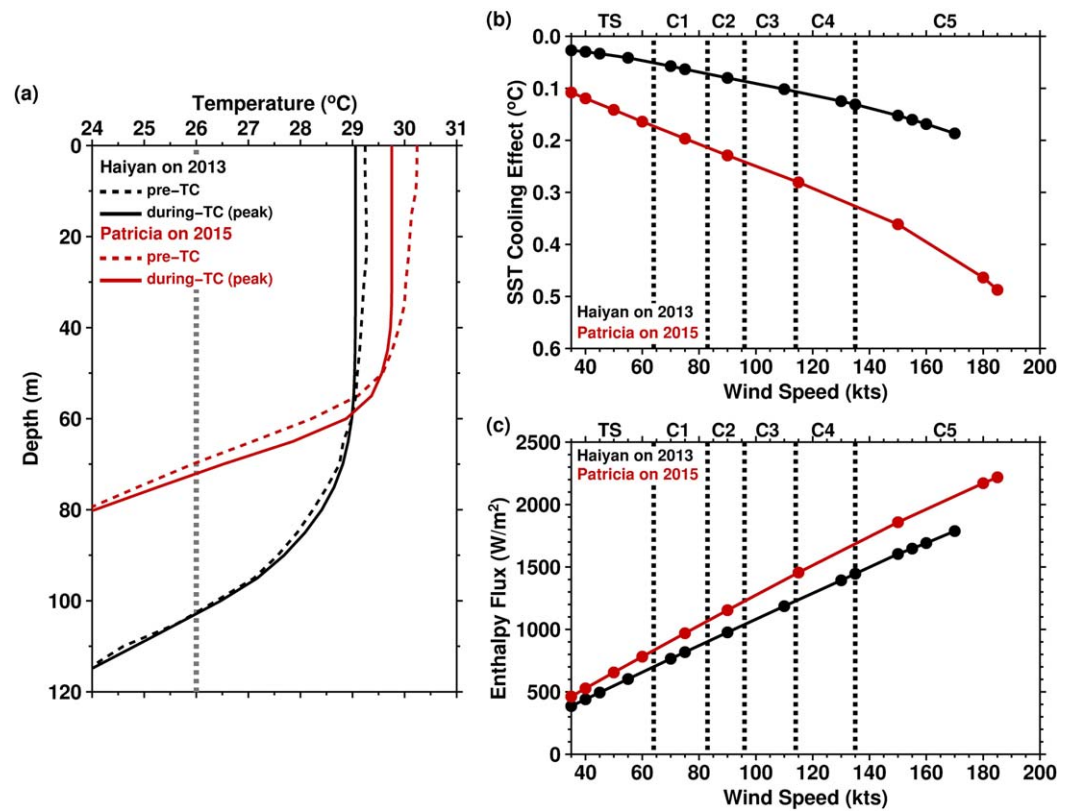


**Figure 2.** The intensification process from Tropical Storm (TS, according to the Saffir-Simpson scale) to Peak for Patricia (red) and Haiyan (black). The below-TCs temperature vertical structures are shown in Figure 2a, dash lines are preexisting ocean conditions averaged from Argo in situ profiles along TC track, and solid lines are ocean conditions at TC peak after cooling effect (calculated from the 3DPWP model). The respective corresponding TC-induced SST cooling effect and inferred enthalpy fluxes estimated from different wind speed (categories) of Patricia and Haiyan are shown in Figures 2b and 2c.

Haiyan) can counterbalance the strong cooling effect (0.5°C for Patricia versus 0.2°C for Haiyan), and also the smaller  $T_a$  (near-surface air temperature) can contribute to larger air-sea temperature differences and resulting in higher sensible heat flux supply. Similarly, for the latent heat flux supply, the key factor is governed by the air-sea humidity difference ( $\Delta q$ ).  $\Delta q$  is calculated as  $[q_s(SST_{mixed}) - q_a]$ , where  $q_a$  is the near-surface air humidity. This results ultimately in stronger enthalpy fluxes (supporting information Figures S2 and S3 and Table 2a) and smaller TCHP differences (despite the significant difference in thermocline depth between Patricia and Haiyan).

**Table 1.** Corresponding to Figures 2–5 and Supporting Information Figures S2–S6, the Preexisting Ocean Conditions From Argo In Situ Float Profiles (a) and Atmospheric Environment Monthly Mean From NCEP/NCAR R1 Reanalysis (b) Along Haiyan and Patricia Trajectories

TC Cases	$SSS_{preTC}$ (g/kg) <sup>a</sup>	$SST_{preTC}$ (°C) <sup>a</sup>	$T100_{preTC}$ (°C) <sup>a</sup>	$TCHP_{preTC}$ (kJ/cm <sup>2</sup> ) <sup>a</sup>	$D26_{preTC}$ (m) <sup>a</sup>	$D20_{preTC}$ (m) <sup>a</sup>
(a) Ocean Preconditions						
Haiyan in Nov 2013	34.2	29.2	28.7	118	103	141
Patricia in Oct 2015	33.3	30.2	27.2	104	70	96
TC Cases	$T_a$ (°C) <sup>b</sup>	$T_d$ (°C) <sup>b</sup>	$q_a$ (g/kg) <sup>b</sup>	$VWS$ (m/s) <sup>b</sup>		
(b) Atmospheric Environment						
Haiyan in Nov 2013	27.9	24.6	18.7	1.8		
Patricia in Oct 2015	28.6	24.7	18.8	2.2		

<sup>a</sup>SSS and SST: sea surface salinity and temperature, T100: upper 100 m average temperature, TCHP: tropical cyclone heat potential, D26 and D20: depth of the 26°C and 20°C isotherms.

<sup>b</sup> $T_a$  and  $T_d$ : near surface temperature and dew-point temperature,  $q_a$ : air specific humidity, and VWS, vertical wind shear, the different in wind between 200 and 850 mb.

**Table 2.** As in Table 1<sup>a</sup>

TC Cases	Air-Sea Interaction at TC Peak							
	SST		$\Delta T$ ( $T_s - T_a$ ) (°C) <sup>b</sup>	SHF( $Q_s$ ) ( $W/m^2$ ) <sup>b</sup>	$q_s$ (g/kg) <sup>b</sup>	$\Delta q$ ( $q_s - q_a$ ) (g/kg) <sup>b</sup>	LHF( $Q_L$ ) ( $W/m^2$ ) <sup>b</sup>	Enthalpy Flux (LHF + SHF) ( $W/m^2$ )
	Cooling Effect (°C) <sup>b</sup>	$SST_{mixed}$ ( $T_s$ ) (°C) <sup>b</sup>						
(a) Haiyan in Nov 2013	0.2	29.1	1.2	144	24.3	5.6	1644	1788
Patricia in Oct 2015	0.5	29.8	1.2	152	25.3	6.5	2066	2218
(b) Patricia in Oct 2015 (increase TC $U_h$ )	0.4	29.9	1.3	167	25.4	6.6	2118	2285
Patricia in Oct 2015 (increase TC size)	1.6	28.6	0.0	3	23.7	4.9	1558	1561
(c) Patricia in Oct 2015 (change latitude (f))	0.5	29.8	1.2	152	25.3	6.5	2068	2220
(d) Patricia in Oct 2015 (change salinity)	0.5	29.7	1.1	144	25.2	6.4	2037	2181

<sup>a</sup>(a) Corresponding to Figure 2 and supporting information Figures S2 and S3, the TC-induced ocean cooling effect,  $SST_{mixed}$ ,  $q_s$ , atmospheric and ocean temperature and humidity differences ( $\Delta T$ ,  $\Delta q$ ), and air-sea enthalpy flux (SHF and LHF) from the cooling effect at the lifetime peak of Haiyan and Patricia. (b) Corresponding to Figure 3 and supporting information Figure S4 and S5, as in Table 2a, but conducted from two additional sensitivity experiments: (1) increased Patricia's translation speed ( $U_h$ ) as fast as Haiyan (blue) and (2) increased Patricia's size as large as Haiyan (green). The TC translation speed and TC size are indicated in supporting information Table S1. (c) Corresponding to Figure 4, as in Table 2a, but with changed the latitude of Patricia similar to Haiyan's (from 14.4°N to 7.4°N) (blue). (d) Corresponding to Figure 5, as in Table 2a, but with increased Patricia's preexisting ocean salinity, similar to Haiyan's condition (blue). The preexisting salinity is shown in Table 1a.

<sup>b</sup>SST cooling effect: TC-induced ocean cooling effect, and averaged over and area of 2.5 times radius of RMW,  $SST_{mixed}(T_s)$ ; during-TC SST,  $q_s$ : surface specific humidity of  $T_s$ , and SHF and LHF: sensible and latent heat flux respective governed by  $\Delta T$  and  $\Delta q$ .

To explore further the differences in cooling effect between Patricia and Haiyan, we conduct additional sensitivity experiments, to quantify the possible influence of different storms' size and translation speed (shown in supporting information Table S1). As summarized in the results in Figure 3, supporting information Figures S4 and S5, and Tables 2a and 2b, the smaller ocean cooling effect of Haiyan is a result of its very deep and warm preexisting ocean subsurface thermal condition and fast translation speed [Lin *et al.*, 2014]. However, Patricia's size was smaller than Haiyan, thus could partially cancel the stronger cooling effect, due to the difference in the subsurface thermal condition and translation speed. In Figure 3, supporting information Figures S4 and S5, and Table 2b, we observed an increased SST cooling effect if Patricia size was similar to Haiyan's (Figure 3, green line). As in Lin [2012], the larger the TC size, the longer the time for a point in the ocean to experience the intense TC wind, the stronger ocean cooling corresponds. We also simulated air-sea condition if Patricia translation speed was as fast as Haiyan's (i.e., increased from  $U_h = 6.2\text{--}8.4$  m/s). In such a scenario, Patricia's cooling effect would decrease by about 0.4°C (comparing red and blue lines in Figure 3b and supporting information Figure S4a). Otherwise, we also consider the effect of the upwelling velocity between different locations (i.e., latitude). As in Figure 4 and Table 2c, Patricia's cooling effect almost have no difference when it pass through the same range of latitude with Haiyan's (comparing red and blue lines in Figure 4, under  $U_h = 6.2$  m/s). Although the upwelling strength is depend on  $f$  (Coriolis parameter) according to latitude, but if the hurricane moves very fast, then  $f$  effect may become less important. Here we also test under a slower translation speed ( $U_h = 1$  m/s), the different cooling results can be seen (supporting information Figure S6).

Finally, we diagnose the potential differences in preexisting ocean salinity conditions between the two TCs. Salinity has been shown to be influential on TC intensification through the presence of quasi-permanent salinity-induced barrier layers in the tropical oceans [Balaguru *et al.*, 2012; Zhang *et al.*, 2017]. They are defined as the layer between the mixed layer depth and the isothermal layer depth. When TCs pass over regions with such oceanic features (abundantly present in the Eastern Pacific), the increased stratification and stability can reduce the storm-induced vertical mixing and SST cooling. Results suggest however little difference in salinity characteristics between Patricia and Haiyan (Figure 5 and Table 2d), although it has been shown that salinity did play a role in Patricia's intensification [Foltz and Balaguru, 2016]. It should also be clarified that during both Patricia and Haiyan lifetime, local conditions were much more favorable than usual (climatological), as already reported in existing literature [Lin *et al.*, 2014; Foltz and Balaguru, 2016]. In short, Haiyan's environment was characterized by preexisting warm SST, thick warm subsurface layer, fast translation speed, larger TC size and relatively higher salinity. Patricia's environment was characterized by preexisting extremely warm SST, shallower subsurface warm layer, slower translation speed, smaller TC size and slightly lower salinity. Our results here focus on comparing the local environment between these two exceptional TCs. They essentially indicate that deeper preexisting ocean conditions associated with a faster translation speed resulted in a smaller SST cooling effect during Haiyan than during Patricia [Lin *et al.*, 2014]

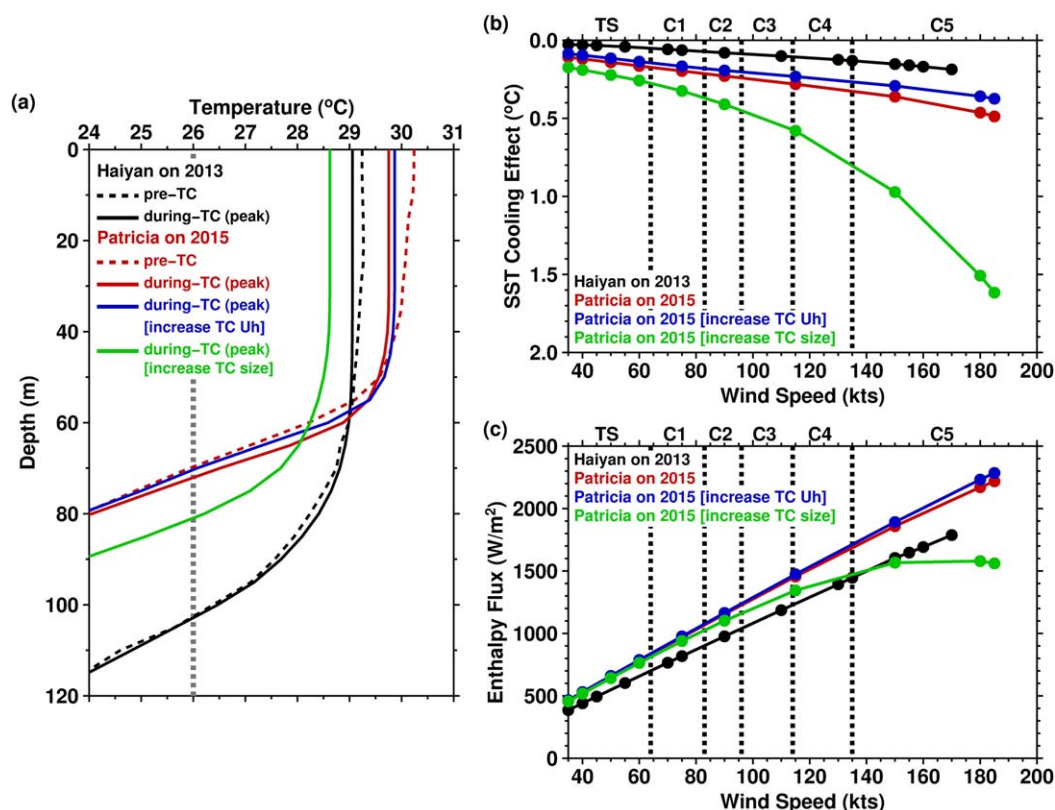


**Figure 3.** Same as Figure 2, but conducted with two additional sensitivity experiments: (1) increased Patricia's translation speed ( $U_h$ ) as fast as Haiyan (blue line) and (2) increased Patricia's size as large as Haiyan (green line). The TC translation speed and TC size are indicated in supporting information Table S1.

(Figure 3, supporting information Figures S4 and S5, and Table 2). Although Patricia's cooling effect was larger, it was well absorbed by the extremely warm  $SST_{preTC} > 30^\circ C$ , that contributed to a larger difference in air-sea temperature and humidity ( $\Delta T$  and  $\Delta q$ ), and subsequently to a larger air-sea enthalpy flux available for Patricia's rapid intensification.

#### 4. Air-Sea Flux for Patricia Under Six Different ENSO Conditions

Recently, a study by *Boucharel et al.* [2016a] emphasized the different controls of TC activity in the Eastern Pacific by different types and phases of ENSO. The oceanic control, through meridional redistribution of subsurface heat, is the main driver of TC activity during the hurricane season following EP El Niño events [*Jin et al.*, 2014], while the altered atmospheric circulation, especially the reduction of vertical wind shear and the increase in relative humidity, tends to be more influential in controlling the hurricane activity after the peak of CP El Niño and La Niña events [*Boucharel et al.*, 2016a]. Hurricane Patricia formed and intensified during the buildup of the strongest EP El Niño ever recorded and it is intriguing to assess to which extent the large-scale and local environmental conditions associated with this particular phase and mode of ENSO participated in the storm's rapid and intense strengthening.

In this section, following a similar approach as the one by *Boucharel et al.* [2016a], we simulated the air-sea enthalpy flux under six different ENSO scenarios: EP El Niño developing and decaying summers, CP El Niño developing and decaying summers, La Niña developing summer, and long-term climatological summer conditions. For each "scenario," we select and compose the three most representative years (indicated in Table 3) following the classification by NOAA based on the Oceanic Niño Index while the climatological conditions are inferred from the seasonal summer averaged over the period 1980–2015 [*Yu et al.*, 2012]. We then compare the 2015 "Patricia conditions" to the idealized conditions associated with each of these ENSO scenarios, in particular during the latest stage of the storm development (from Tropical Storm (TS)

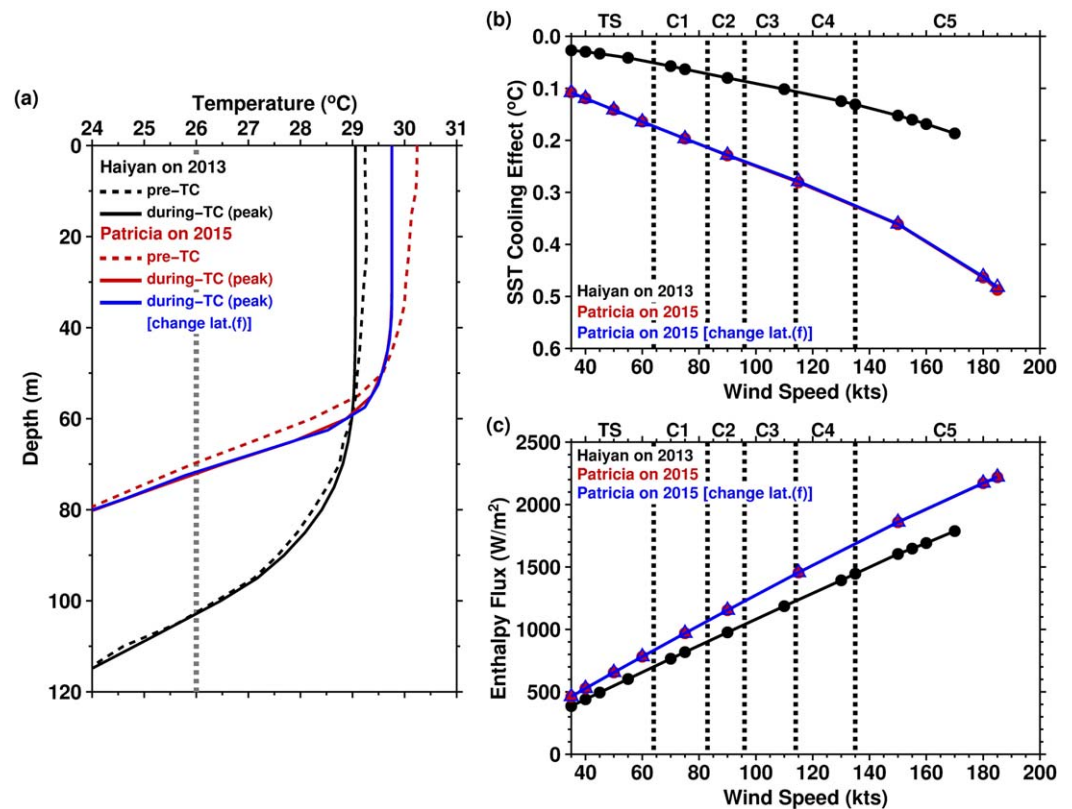


**Figure 4.** Same as Figure 2, but conducted with another sensitivity experiments: change the latitude of Patricia’s location from 14.4°N to 7°N (as Haiyan’s) (blue line).

(102100Z, 35 knots) to Peak (102312Z, 185 knots). Note that we expand the analysis by *Boucharel et al.* [2016a] by comparing typical ENSO conditions not only after the peak but also during the buildup of the event.

Figure 6a shows the pre-TC oceanic vertical thermal structure in the region of Patricia influence for these six different conditions: developing (magenta line), decaying (orange line) EP El Niño, developing (golden line), decaying (green line) CP El Niño, La Niña (blue line), and climatological conditions (black line). Consistently with the findings of *Boucharel et al.* [2016a], we find warmer (respectively colder) subsurface conditions than the long-term climatology in October for the decaying EP (respectively CP) El Niño, therefore favorable (respectively detrimental) to hurricane intensification. La Niña conditions are also characterized by weaker heat content in the region of Patricia intensification, therefore also unfavorable to TC growth. Interestingly, the subsurface oceanic properties are much warmer during the buildup of EP El Niño events than during the following season, when yet the ENSO equatorial heat is already discharged into the Eastern Pacific TC region [*Jin et al.*, 2014]. However, a close look at the spatial patterns of the first two EOF modes of heat content variability in the Eastern Pacific (their Figure 1) shows that in the region where Patricia developed (just off the coast of Mexico), the “discharge mode” (EOF2) has no signature. The subsurface heat is actually mostly discharged further into the central Eastern Pacific. In contrast, the first EOF mode, representative of El Niño growth and peak, exhibits warmer heat content close to the coast in this area. The EP El Niño has a strong heat content signature in this region during the buildup of the event until the boreal winter peak (Figure 6a, magenta line), therefore providing very favorable subsurface conditions for hurricane development. Note that the 2015 EP El Niño displays a much warmer subsurface temperature than the typical EP El Niño event. Such particular buildup conditions are therefore even more favorable to TC intensification. Additionally, the buildup of CP El Niño events is slightly favorable to hurricane growth in the Eastern Pacific coastal region. We carry on the analysis by comparing the SST cooling factors inferred from the 3D-PWP model from these six different ENSO conditions. And unsurprisingly, the 2015, developing EP El Niño, decaying EP El Niño, and developing CP El Niño conditions all display reduced SST cooling (in that order) in this

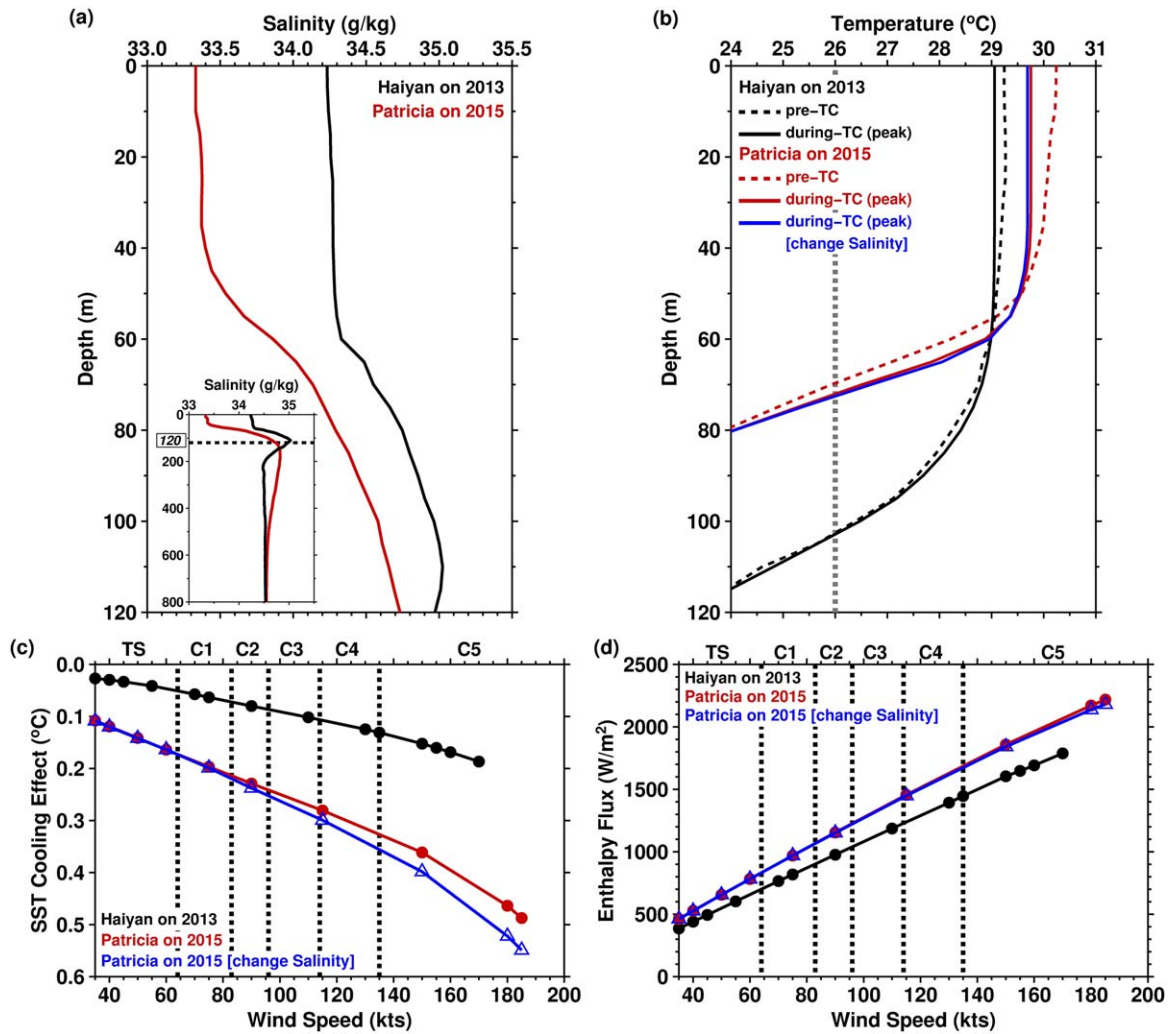


**Figure 5.** (b–d) The same as Figures 2a–c, but calculated using increased Patricia’s preexisting ocean salinity condition to be similar to Haiyan’s (blue line). The preexisting ocean salinity vertical structure from Argo profiles along Patricia (red) and Haiyan (black) are shown in Figure 5a, and Table 1a.

region, in particular for the strongest wind speeds related to hurricane of Category 3 and above; as opposed to the decaying CP El Niño and La Niña conditions, which both show a substantial increase in SST cooling compared to the climatology.

Figure 6c and Table 3 summary the enthalpy flux results under these different conditions (solid lines). With a weaker SST cooling under developing EP El Niño, decaying EP El Niño, and developing CP El Niño (Figure 6b), such ENSO characteristics are able to provide more enthalpy flux (~1500–1600 W/m<sup>2</sup>) favorable for TC intensification. The other three conditions (including climatology) are rather unfavorable, with 30–70% reduction in enthalpy flux supply in comparison. However, the potential flux supply of the three most favorable ENSO conditions remains 37% smaller than the one observed during the 2015 Patricia conditions (~2100 W/m<sup>2</sup>, Figure 6, red solid line). This suggests that Patricia’s extraordinary intensity may not be achievable under any of these typical ENSO conditions. In other words, the 2015 summer was characterized by extraordinary EP El Niño conditions, i.e., extremely favorable local and large-scale environmental conditions leading to an intense TC season and in particular to the development of a record-breaking hurricane.

To go deeper into our analysis, we evaluate the relative influence of atmospheric versus oceanic conditions on the strength of air-sea enthalpy fluxes. We compute such fluxes using respective oceanic properties from all six different ENSO scenarios coupled with the same climatological atmospheric environments (dashed lines in Figure 6 and supporting information Figures S7 and S8). Once again, apart for La Niña and

**Table 3.** Corresponding to Figure 6 and Supporting Information Figures S7 and S8, the Preexisting Ocean Conditions From GODAS Reanalysis Monthly Mean Data (a) and Atmospheric Environment From NCEP/NCAR R1 Reanalysis Monthly Mean Data (b) Along Patricia Trajectories in October 2015 and for Different Types of ENSO Conditions<sup>a</sup>

Patricia in Different ENSO Conditions: Years	SST <sub>preTC</sub> (°C)	T100 <sub>preTC</sub> (°C)	TCHP <sub>preTC</sub> (kJ/cm <sup>2</sup> )	D26 <sub>preTC</sub> (m)	D20 <sub>preTC</sub> (m)			
<b>(a) Ocean Preconditions</b>								
2015	30.0	27.0	101	70	92			
EP developing : 1982, 1991, 1997	28.7	24.3	46	50	76			
EP decaying : 1983, 1992, 1998	28.8	24.6	47	52	79			
CP developing : 2002, 2004, 2009	29.5	23.2	50	43	64			
CP decaying : 2003, 2005, 2010	28.6	21.4	22	28	56			
La Niña : 1988, 1999, 2010	28.0	20.7	16	24	49			
Clima : 1980~2015	28.8	22.7	30	36	64			
Patricia in Different ENSO Conditions: Years	T <sub>a</sub> (°C)	T <sub>d</sub> (°C)	q <sub>a</sub> (g/kg)	VWS (m/s)				
<b>(b) Atmospheric Environment</b>								
2015	28.6	24.7	18.8	2.2				
EP developing : 1982, 1991, 1997	27.6	23.9	17.9	3.6				
EP decaying : 1983, 1992, 1998	27.7	24.0	18.0	3.1				
CP developing : 2002, 2004, 2009	28.0	24.0	18.0	2.9				
CP decaying : 2003, 2005, 2010	27.6	23.4	17.4	5.4				
La Niña : 1988, 1999, 2010	27.4	23.4	17.3	6.8				
Clima : 1980~2015	27.8	23.9	17.9	4.1				
Patricia in Different ENSO Conditions: Years	SST Cooling Effect (°C)	SST <sub>mixed</sub> (T <sub>s</sub> ) (°C)	ΔT (T <sub>s</sub> -T <sub>a</sub> ) (°C)	SHF (Q <sub>s</sub> ) (W/m <sup>2</sup> )	q <sub>s</sub> (g/kg)	Δq(q <sub>s</sub> - q <sub>a</sub> ) (g/kg)	LHF (Q <sub>l</sub> ) (W/m <sup>2</sup> )	Enthalpy Flux (LHF + SHF) (W/m <sup>2</sup> )
<b>(c) Air-Sea Interaction at TC Peak</b>								
2015	0.4	29.6	1.0	131	25.0	6.2	1992	2122
EP developing : 1982, 1991, 1997	0.8	27.9	0.2	32	22.6	4.7	1521	1553
EP decaying : 1983, 1992, 1998	0.9	27.9	0.2	22	22.6	4.6	1490	1512
CP developing : 2002, 2004, 2009	1.2	28.2	0.3	34	23.1	5.2	1655	1688
CP decaying : 2003, 2005, 2010	2.2	26.4	-1.1	-152	20.8	3.4	1087	935
La Niña : 1988, 1999, 2010	2.4	25.6	-1.9	-247	19.7	2.4	783	537
Clima : 1980~2015	1.7	27.1	-0.6	-85	21.6	3.8	1210	1124

<sup>a</sup>(c) Shows the corresponding TC-induced ocean cooling effect, SST<sub>mixed</sub>, q<sub>s</sub>, atmospheric and ocean temperature and humidity differences (ΔT, Δq), and air-sea enthalpy flux (SHF and LHF) from the cooling effect at the lifetime peak of Patricia.

the decaying CP El Niño conditions, all other ENSO types and phases show increased enthalpy fluxes in climatological atmospheric environments too. This confirms the major contribution by ocean surface and subsurface properties in providing favorable air-sea coupling for the intensification of major hurricanes and suggests that climatological atmospheric environments would partially offset the ocean's positive contributions to TCs intensification. These results also support *Boucharel et al.* [2016a] conclusions of a more dominant control of atmospheric environmental factors in the growth of major TCs decaying CP and La Niña events.

We finally explore the role of a crucial large-scale atmospheric dynamic factor in TCs intensification, namely the vertical wind shear (VWS). As summarized in Table 3b, the three most favorable ENSO conditions in terms of air-sea enthalpy fluxes (developing EP, decaying EP, and developing CP) are also accompanied by lower VWS, i.e., more favorable to storm strengthening, in particular in October 2015. As the 2015 El Niño became the most intense EP El Niño ever observed [*Jacox et al.*, 2016], it seems natural to compare the air-sea fluxes conditions to those that accompanied the buildup of the two previous record-holders: the 1982 and 1997 EP El Niño (supporting information Figures S9–S12 and supporting information Table S2). Supporting information Figure S10a compares the Argo floats with the GODAS reanalysis data and both display a very similar vertical thermal structure, which entrusts us in using GODAS data for the earlier years before the Argo era (i.e., 1982 and 1997). Again, the SST and subsurface ocean conditions in October 2015 stand out among the three strong EP developing years (supporting information Figures S9 and S10a) and the flux supply for 2015 was above 2000 W/m<sup>2</sup> compared to ~1500 W/m<sup>2</sup> supply for 1997 and 1982 (supporting information Figure S10c and supporting information Table S2c). This again highlights the unprecedentedly warm oceanic characteristics in October 2015 that contributed to Hurricane Patricia's extraordinary intensification.

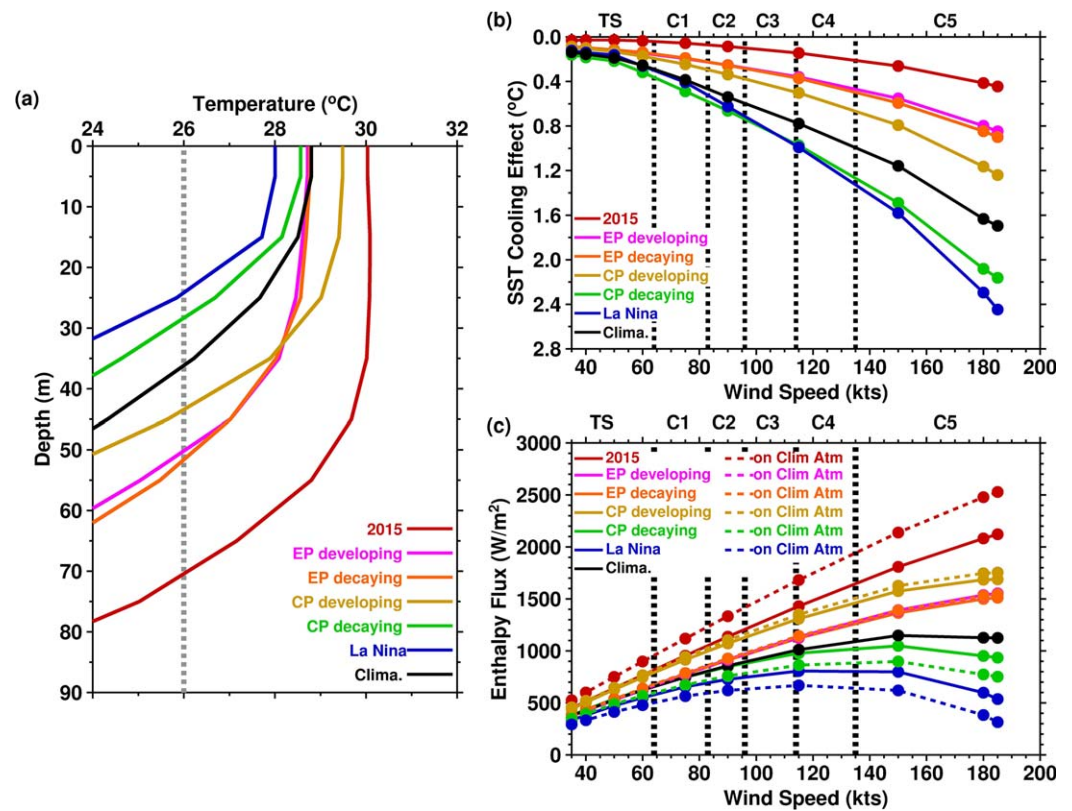


**Figure 6.** Intensification process from Tropical Storm (TS) to Peak of Patricia in October 2015 (red solid line) for different types of ENSO events: EP developing year (magenta solid line), EP decaying year (orange solid line), CP developing year (golden solid line), CP decaying year (green solid line), La Niña (blue solid line), and also for the climatological conditions (black solid line). (a) The pre-TC oceanic vertical thermal structure from GODAS monthly mean reanalysis along Patricia track. The respective corresponding TC-induced SST cooling effect and enthalpy fluxes estimated for different wind speeds (categories) are shown respectively in Figures 6b and 6c. The dashed lines in Figure 6c represent the enthalpy fluxes for the six different ENSO cases but calculated using their respective climatological atmospheric environments.

## 5. Discussion and Conclusion

By combining a variety of data sets, ranging from Argo profilers to reanalysis products, we studied the thermodynamical processes that led to the exceptional intensification of Hurricane Patricia in October 2015 in the Eastern Pacific with a special emphasis on the air-sea enthalpy flux conditions and a comparison with supertyphoon Haiyan (2013). Patricia reached the extraordinary maximum wind speed of 185 knots making it the strongest hurricane ever recorded, above supertyphoon Haiyan that devastated the Philippines in October 2013 [Lin et al., 2014; Lander et al., 2014; Takagi et al., 2016; Rogers et al., 2017]. After the recent TC Winston in March 2016 that strongly impacted the Fiji Islands with wind speed surpassing 155 knots, this boosts the scientific community to study and assess the physical mechanisms that cause such dramatic storm intensification and ultimately the formation of “super hurricanes.”

We find that Patricia was characterized by a higher enthalpy flux supply than Haiyan, despite a larger storm-induced ocean cooling effect (0.5°C versus 0.2°C for Haiyan). This is explained by Patricia’s much warmer pre-TC sea surface temperature ( $SST_{preTC} = 30.2^\circ\text{C}$  versus  $29.2^\circ\text{C}$  for Haiyan), which counterbalanced the SST cooling effect and lead to a warmer mixed SST during Patricia’s passing ( $SST_{mixed} = 29.8^\circ\text{C}$  versus  $29.1^\circ\text{C}$  for Haiyan). As a result, there were larger air-sea temperature and humidity differences at the TC’s air-ocean interface that contributed to a 24% larger enthalpy (sensible and latent heat) fluxes available for Patricia’s intensification (2218 versus 1788  $\text{W}/\text{m}^2$  for Haiyan). Additionally, we find that moderately favorable dynamical atmospheric properties, especially a reduced vertical wind shear, also may have contributed to the exceptional intensification of Hurricane Patricia. We further diagnosed four potential contributing factors to Patricia’s larger TC-induced cooling effect: the preexisting upper ocean temperature profile, ocean salinity effect, TC translation speed and TC size. The two most influential restrictions for Patricia’s

enhancement are the preexisting thermal structure in the Eastern Pacific (characterized by a shallower thermocline depth and a smaller tropical cyclone heat potential than Haiyan) and a slower storm's translation speed.

To complement our analysis of Patricia's exceptional growth, we simulated the air-sea enthalpy flux supply if the storm had developed under six different climate conditions associated with different phases or modes of ENSO (i.e., Eastern Pacific (EP) and Central Pacific (CP) El Niño developing and decaying summers, La Niña developing summer and long-term climatological summer condition). We found that the EP developing and decaying summer, and the CP developing summer are the three most favorable scenarios for major TCs intensification, contributing to  $\sim 1500\text{--}1600\text{ W/m}^2$  air-sea enthalpy fluxes. Although 2015 was an EP El Niño developing summer, its enthalpy flux supply reached  $2100\text{ W/m}^2$ , representing a 37% increase from the typical EP summertime development. This highlights the exceptional characteristics of the 2015 TC season associated with the buildup of an extreme El Niño event in the Eastern Pacific, which allowed Patricia to reach its extraordinary intensity.

This paper confirms and supplements recent studies on the dominant control of oceanic subsurface properties on the modulation of TC intensity in the Eastern Pacific [Balaguru *et al.*, 2013; Vincent *et al.*, 2014], and in particular related to ENSO dynamics [Jin *et al.*, 2014, 2015; Boucharel *et al.*, 2016a,2016c]. These studies focused on the delayed ENSO effect associated with the meridional heat discharge into the TC region that follows the wintertime peak of El Niño, therefore available for TC intensification during the next boreal hurricane season. In this research, we highlighted that not only the EP decaying year, but also both EP and CP El Niño buildup can provide favorable surface and subsurface conditions for hurricane intensification in particular along the coast of the Americas, though not a result of the ENSO recharge-discharge process [Jin, 1997; Jin *et al.*, 2014]. Boucharel *et al.* [2016b] suggested that the exceptional intensity of the 2015 TC season in the Eastern Pacific and its subseasonal modulation was linked to the propagation of intraseasonal equatorial Kelvin waves (that triggered the 2015 EP El Niño) and their effect on the thermocline depth and heat content anomalies [Foltz and Balaguru, 2016]. Murakami *et al.* [2017] have also reported the very active TC season in 2015, with linkage not only related to El Niño, but possibly to other climate modes, such as the Pacific meridional mode [Chang *et al.*, 2007].

#### Acknowledgments

This work is supported by Taiwan's Ministry of Science and Technology (MOST) under grant NSC 103-2111-M-002-002-MY3. Thanks to the Argo (<https://data.nodc.noaa.gov/argo/data/>) and NOAA/NCEP (<https://www.esrl.noaa.gov/psd/data/gridded/data.ncep.reanalysis.html>) for providing essential data sets, and to NHC (<http://ftp.nhc.noaa.gov/atcf/archive/>) and JTWC ([https://metoc.ndbc.noaa.gov/web/guest/jtwc/best\\_tracks/](https://metoc.ndbc.noaa.gov/web/guest/jtwc/best_tracks/)) for TC's best track and intensity data. Thanks to the two reviewers for their constructive comments and helpful suggestions on an earlier version of the manuscript.

#### References

- Balaguru, K., P. Chang, R. Saravanan, L. R. Leung, Z. Xu, M. Li, and J. S. Hsieh (2012), Ocean barrier layers' effect on tropical cyclone intensification, *Proc. Natl. Acad. Sci.*, *109*(36), 14,343–14,347, doi:10.1073/pnas.1201364109.
- Balaguru, K., R. L. Leung, and J. H. Yoon (2013), Oceanic control of northeast Pacific hurricane activity at interannual timescales, *Environ. Res. Lett.*, *8*(4), 044009, doi:10.1088/1748-9326/8/4/044009.
- Bell, G. D., M. S. Halpert, R. C. Schnell, R. W. Higgins, J. Lawrimore, V. E. Kousky, R. Tinker, W. Thiaw, M. Chelliah, and A. Artusa (2000), Climate assessment for 1999, *Bull. Amer. Meteor. Soc.*, *81*(6), S1–S50, doi:10.1175/1520-0477(2000)81[s1:CAF]2.0.CO;2.
- Bender, M. A., and I. Ginis (2000), Real case simulation of hurricane-ocean interaction using a high-resolution coupled model: Effects on hurricane intensity, *Mon. Weather Rev.*, *128*(4), 917–946, doi:10.1175/1520-0493(2000)128 < 0917:RCSOHO > 2.0.CO;2.
- Black, P. G., E. A. D'Asaro, W. M. Drennan, J. R. French, P. P. Niller, T. B. Sanford, E. J. Terrill, E. J. Walsh, and J. A. Zhang (2007), Air-sea exchange in hurricanes—Synthesis of observations from the coupled boundary layer air-sea transfer experiment, *Bull. Am. Meteorol. Soc.*, *88*(3), 357–374, doi:10.1175/BAMS-88-3-357.
- Bond, N. A., M. F. Cronin, H. Freeland, and N. Mantua (2015), Causes and impacts of the 2014 warm anomaly in the NE Pacific, *Geophys. Res. Lett.*, *42*, 3414–3420, doi:10.1002/2015GL063306.
- Boucharel, J., F. F. Jin, I. I. Lin, H. C. Huang, and M. H. England (2016a), Different control of tropical cyclone activity in the eastern Pacific for two types of El Niño, *Geophys. Res. Lett.*, *43*, 1679–1689, doi:10.1002/2016GL067728.
- Boucharel, J., F. F. Jin, M. E. England, B. Dewitte, I. I. Lin, H. C. Huang, and M. A. Balmaseda (2016b), Influence of oceanic intraseasonal Kelvin waves on the Eastern Pacific hurricane activity, *J. Clim.*, *29*(22), 7941–7955, doi:10.1175/JCLI-D-16-0112.1.
- Boucharel, J., F. F. Jin, M. E. England, and I. I. Lin (2016c), Modes of hurricane activity variability in the Eastern Pacific: Implications for the 2016 season, *Geophys. Res. Lett.*, *43*, 11,358–11,366, doi:10.1002/2016GL070847.
- Camargo, S. J., and A. H. Sobel (2005), Western North Pacific tropical cyclone intensity and ENSO, *J. Clim.*, *18*(15), 2996–3006, doi:10.1175/JCLI3457.1.
- Chang, P., L. Zhang, R. Saravanan, D. J. Vimont, J. C. H. Chiang, L. Ji, H. Seidel, and M. K. Tippett (2007), Pacific meridional mode and El Niño—Southern Oscillation, *Geophys. Res. Lett.*, *34*, L16608, doi:10.1029/2007GL030302.
- Chang, S. W., and R. A. Anthes (1978), Numerical simulations of the ocean's nonlinear, baroclinic response to translating hurricanes, *J. Phys. Oceanogr.*, *8*(3), 468–480, doi:10.1175/1520-0485(1978)008 < 0468:NSOTON > 2.0.CO;2.
- Chu, P. S., and J. Wang (1997), Tropical cyclone occurrences in the vicinity of Hawaii: Are the differences between El Niño and non-El Niño years significant?, *J. Clim.*, *10*(10), 2683–2689, doi:10.1175/1520-0442(1997)010 < 2683:TCOITV > 2.0.CO;2.
- Cione, J. J., E. A. Kalina, J. A. Zhang, and E. W. Uhlhorn (2013), Observations of air-sea interaction and intensity change in hurricanes, *Mon. Weather Rev.*, *141*(7), 2368–2382, doi:10.1175/MWR-D-12-00070.1.
- Comiso, J. C., G. J. P. Perez, and L. V. Stock (2015), Enhanced Pacific Ocean sea surface temperature and its relation to Typhoon Haiyan, *J. Environ. Sci. and Manage.*, *18*(1), 1–10.

- DeMaria, M. (1996), The effect of vertical shear on tropical cyclone intensity change, *J. Atmos. Sci.*, *53*(14), 2076–2087, doi:10.1175/1520-0469(1996)053<2076:TEOVSO>2.0.CO;2.
- Emanuel, K. A. (1986), An air-sea interaction theory for tropical cyclones. Part I: Steady-state maintenance, *J. Atmos. Sci.*, *43*(6), 585–605, doi:10.1175/1520-0469(1986)043<0585:AASITF>2.0.CO;2.
- Emanuel, K. A. (1999), Thermodynamic control of hurricane intensity, *Nature*, *401*(6754), 665–669, doi:10.1038/44326.
- Emanuel, K. A., C. DesAutels, C. Holloway, and R. Korty (2004), Environmental control of tropical cyclone intensity, *J. Atmos. Sci.*, *61*(7), 843–858, doi:10.1175/1520-0469(2004)061<0843:ECOTCI>2.0.CO;2.
- Foltz, G. R., and K. Balaguru (2016), Prolonged El Niño conditions in 2014–15 and the rapid intensification of Hurricane Patricia in the eastern Pacific, *Geophys. Res. Lett.*, *43*, 10,347–10,355, doi:10.1002/2016GL070274.
- Frank, W. M., and E. A. Ritchie (1999), Effects of environmental flow upon tropical cyclone structure, *Mon. Weather Rev.*, *127*(9), 2044–2061, doi:10.1175/1520-0493(1999)127<2044:EOEFUT>2.0.CO;2.
- Frank, W. M., and E. A. Ritchie (2001), Effects of vertical shear on the intensity and structure of numerically simulated hurricanes, *Mon. Weather Rev.*, *129*(9), 2249–2269, doi:10.1175/1520-0493(2001)129<2249:EOVWSO>2.0.CO;2.
- Fu, D., P. Chang, and C. M. Patricola (2017), Intrabasin variability of East Pacific tropical cyclones during ENSO regulated by central American gap winds, *Sci. Rep.*, *7*(1), 1658, doi:10.1038/s41598-017-01962-3.
- Goni, G. J., and J. A. Trinanes (2003), Ocean thermal structure monitoring could aid in the intensity forecast of tropical cyclones, *Eos Trans. AGU*, *84*(51), 573–578, doi:10.1029/2003EO510001.
- Goni, G. J., et al. (2009), Applications of satellite-derived ocean measurements to tropical cyclone intensity forecasting, *Oceanography*, *22*(3), 190–197, doi:10.5670/oceanog.2009.78.
- Goni, G. J., J. A. Knaff, and H. Lin (2011), State of the climate report for 2010: Chapter 4: The Tropics, edited by H. J. Diamond, Section e: Tropical Cyclone Heat Potential, *Bull. Amer. Meteor. Soc.*, *92*(6), S132–S134, doi:10.1175/1520-0477-92.6.S1.
- Gray, W. M. (1979), Hurricanes: Their formation, structure and likely role in the tropical circulation, in *Meteorology Over the Tropical Oceans*, edited by D. B. Shaw, pp. 155–218, R. Meteorol. Soc., Bracknell, Berkshire, U. K.
- Huang, P., I. I. Lin, C. Chou, and R. H. Huang (2015), Change in ocean subsurface environment to suppress tropical cyclone intensification under global warming, *Nat. Commun.*, *6*, 7188, doi:10.1038/ncomms8188.
- Jacox, M. G., E. L. Hazen, K. D. Zaba, D. L. Rudnick, C. A. Edwards, A. M. Moore, and S. J. Bograd (2016), Impacts of the 2015–2016 El Niño on the California Current System: Early assessment and comparison to past events, *Geophys. Res. Lett.*, *43*, 7072–7080, doi:10.1002/2016GL069716.
- Jauregui, E. (2003), Climatology of landfalling hurricanes and tropical storms in Mexico, *Atmósfera*, *16*(4), 193–204.
- Jin, F. F. (1997), An equatorial ocean recharge paradigm for ENSO. Part I: Conceptual model, *J. Atmos. Sci.*, *54*(7), 811–829, doi:10.1175/1520-0469(1997)054<0811:AEORPF>2.0.CO;2.
- Jin, F. F., J. Boucharel, and I. I. Lin (2014), Eastern Pacific tropical cyclones intensified by El Niño delivery of subsurface ocean heat, *Nature*, *516*(7529), 82–85, doi:10.1038/nature13958.
- Jin, F. F., J. Boucharel, and I. I. Lin (2015), El Niño and intense tropical cyclones (Replying to I.-J. Moon, S.-H. Kim, and C. Wang), *Nature*, *526*(7575), E4–E5, doi:10.1038/nature15546.
- Johnson, N. C. (2013), How many ENSO flavors can we distinguish?, *J. Clim.*, *26*(13), 4816–4827, doi:10.1175/JCLI-D-12-00649.1.
- Kaplan, J., and M. DeMaria (2003), Large-scale characteristics of rapidly intensifying tropical cyclones in the North Atlantic basin, *Weather Forecasting*, *18*(6), 1093–1108, doi:10.1175/1520-0434(2003)018<1093:LCORIT>2.0.CO;2.
- Kimberlain, T. B., E. S. Blake, and J. P. Cangialosi (2016), Hurricane Patricia, *National Hurricane Center Tropical Cyclone Report*, NOAA, NWS.
- Kug, J. S., F. F. Jin, and S. I. An (2009), Two types of El Niño events: Cold tongue El Niño and warm pool El Niño, *J. Clim.*, *22*(6), 1499–1515, doi:10.1175/2008JCLI2624.1.
- Lander, M., C. Guard, and S. J. Camargo (2014), Tropical cyclones, Super Typhoon Haiyan, in State of the Climate in 2013, *Bull. Amer. Meteor. Soc.*, *95*(7), S112–S114, doi:10.1175/2014BAMSStateoftheClimate.1.
- Lin, I. I. (2012), Typhoon-induced phytoplankton blooms and primary productivity increase in the western North Pacific subtropical ocean, *J. Geophys. Res.*, *117*, C03039, doi:10.1029/2011JC007626.
- Lin, I. I., C. C. Wu, K. Emanuel, I. H. Lee, C.-R. Wu, and I.-F. Pun (2005), The interaction of Supertyphoon Maemi (2003) with a warm ocean eddy, *Mon. Weather Rev.*, *133*(9), 2635–2649, doi:10.1175/MWR3005.1.
- Lin, I. I., C. C. Wu, I. F. Pun, and D. S. Ko (2008), Upper-ocean thermal structure and the western North Pacific category-5 typhoons: Part I: Ocean features and the category 5 typhoons' intensification, *Mon. Weather Rev.*, *136*(9), 3288–3306, doi:10.1175/2008MWR2277.1.
- Lin, I. I., C. H. Chen, I. F. Pun, W. T. Liu, and C. C. Wu (2009a), Warm ocean anomaly, air sea fluxes, and the rapid intensification of tropical cyclone Nargis (2008), *Geophys. Res. Lett.*, *36*, L03817, doi:10.1029/2008GL035815.
- Lin, I. I., I. F. Pun, and C. C. Wu (2009b), Upper ocean thermal structure and the western North Pacific category-5 typhoons: Part II: Dependence on translation speed, *Mon. Weather Rev.*, *137*(11), 3744–3757, doi:10.1175/2009MWR2713.1.
- Lin, I. I., G. J. Goni, J. A. Knaff, C. Forbes, and M. M. Ali (2013a), Ocean heat content for tropical cyclone intensity forecasting and its impact on storm surge, *Nat. Hazards*, *66*(3), 1481–1500, doi:10.1007/s11069-012-0214-5.
- Lin, I. I., P. Black, J. F. Price, C. Y. Yang, S. S. Chen, C. C. Lien, P. Harr, N. H. Chi, C. C. Wu, and E. A. D'Asaro (2013b), An ocean coupling potential intensity index for tropical cyclones, *Geophys. Res. Lett.*, *40*, 1878–1882, doi:10.1002/grl.50091.
- Lin, I. I., I. F. Pun, and C. C. Lien (2014), "Category-6" supertyphoon Haiyan in global warming hiatus: Contribution from subsurface ocean warming, *Geophys. Res. Lett.*, *41*, 8547–8553, doi:10.1002/2014GL061281.
- Lin, I. I. and J. C. L. Chan (2015), Recent decrease in typhoon destructive potential and global warming implications, *Nat. Commun.*, *6*, 7182, doi:10.1038/ncomms8182.
- Mainelli, M., M. DeMaria, L. K. Shay, and G. Goni (2008), Application of oceanic heat content estimation to operational forecasting of recent Atlantic category 5 hurricanes, *Weather Forecasting*, *23*(1), 3–16, doi:10.1175/2007WAF2006111.1.
- Mei, W., C. C. Lien, I. I. Lin, and S. P. Xie (2015), Tropical cyclone-induced ocean response: A comparative study of the South China Sea and tropical Northwest Pacific, *J. Clim.*, *28*(15), 5952–5968, doi:10.1175/JCLI-D-14-00651.1.
- Murakami, H., B. Wang, T. Li, and A. Kitoh (2013), Projected increase in tropical cyclones near Hawaii, *Nat. Clim. Change*, *3*(8), 749–754, doi:10.1038/nclimate1890.
- Murakami, H., et al. (2017), Dominant role of subtropical Pacific warming in extreme Eastern Pacific Hurricane seasons: 2015 and the future, *J. Clim.*, *30*(1), 243–264, doi:10.1175/JCLI-D-16-0424.1.
- Nakamura, R., T. Shibayama, M. Esteban, and T. Iwamoto (2016), Future typhoon and storm surges under different global warming scenarios: Case study of typhoon Haiyan (2013), *Nat. Hazards*, *82*(3), 1645–1681, doi:10.1007/s11069-016-2259-3.

- Powell, M. D., P. J. Vickery, and T. A. Reinhold (2003), Reduced drag coefficient for high wind speeds in tropical cyclones, *Nature*, 422(6929), 279–283, doi:10.1038/nature01481.
- Price, J. F. (1981), Upper ocean response to a hurricane, *J. Phys. Oceanogr.*, 11(2), 153–175, doi:10.1175/1520-0485(1981)011<0153:UOR-TAH>2.0.CO;2.
- Price, J. F. (2009), Metrics of hurricane-ocean interaction: Vertically-integrated or vertically-averaged ocean temperature?, *Ocean Sci.*, 5(3), 351–368, doi:10.5194/os-5-351-2009.
- Price, J. F., R. A. Weller, and R. Pinkel (1986), Diurnal cycling: Observations and models of the upper ocean response to diurnal heating, cooling, and wind mixing, *J. Geophys. Res.*, 91(C7), 8411–8427, doi:10.1029/JC091iC07p08411.
- Price, J. F., T. B. Sanford, and G. Z. Forristall (1994), Forced stage response to a moving hurricane, *J. Phys. Oceanogr.*, 24(2), 233–260, doi:10.1175/1520-0485(1994)024<0233:FSRTAM>2.0.CO;2.
- Pun, I. F., I. I. Lin, C. R. Wu, D. S. Ko, and W. T. Liu (2007), Validation and application of altimetry-derived upper ocean thermal structure in the western North Pacific ocean for typhoon-intensity forecast, *IEEE Trans. Geosci. Remote Sens.*, 45(6), 1616–1630, doi:10.1109/TGRS.2007.895950.
- Pun, I. F., Y. T. Chang, I. I. Lin, T. Y. Tang, and R. C. Lien (2011), Typhoon-ocean interaction in the western North Pacific: Part 2, *Oceanogr.*, 24(4), 32–41, doi:10.5670/oceanog.2011.92.
- Pun, I. F., I. I. Lin, and M. H. Lo (2013), Recent increase in high tropical cyclone heat potential area in the Western North Pacific Ocean, *Geophys. Res. Lett.*, 40(17), 4680–4684, doi:10.1002/grl.50548.
- Pun, I. F., I. I. Lin, D. S. Ko (2014), New generation of satellite-derived ocean thermal structure for the western north pacific typhoon intensity forecasting, *Prog. Oceanogr.*, 121, 109–124, doi:10.1016/j.pocean.2013.10.004.
- Raga, G. B., B. Bracamontes-Ceballos, L. M. Farfán, and R. Romero-Centeno (2013), Landfalling tropical cyclones on the Pacific coast of Mexico: 1850–2010, *Atmósfera*, 26(2), 209–220, doi:10.1016/S0187-6236(13)71072-5.
- Ritchie, E. A., K. M. Wood, D. S. Gutzler, and S. R. White (2011), The influence of eastern Pacific tropical cyclone remnants on the southwestern United States, *Mon. Weather Rev.*, 139(1), 192–210, doi:10.1175/2010MWR3389.1.
- Rogers, R. F., S. Aberson, M. M. Bell, D. J. Cecil, J. D. Doyle, T. B. Kimberlain, J. Morgerman, L. K. Shay, and C. Velden (2015), Re-writing the tropical record books: The extraordinary intensification of Hurricane Patricia, *Bull. Amer. Meteor. Soc.*, doi:10.1175/BAMS-D-16-0039.1.
- Scharroo, R., W. H. F. Smith, and J. L. Lillibridge (2005), Satellite altimetry and the intensification of Hurricane Katrina, *Eos Trans. AGU*, 86(40), 366, doi:10.1029/2005EO400004.
- Shay, L. K., G. J. Goni, and P. G. Black (2000), Role of a warm ocean feature on Hurricane Opal, *Mon. Weather Rev.*, 128(5), 1366–1383, doi:10.1175/1520-0493(2000)128<1366:EOAWOF>2.0.CO;2.
- Shu, S., and F. Zhang (2015), Influence of equatorial waves on the genesis of Super Typhoon Haiyan (2013), *J. Atmos. Sci.*, 72(12), 4591–4613, doi:10.1175/JAS-D-15-0016.1.
- Takagi, H., and M. Esteban (2016), Statistics of tropical cyclone landfalls in the Philippines: Unusual characteristics of 2013 Typhoon Haiyan, *Nat. Hazards*, 80(1), 211–222, doi:10.1007/s11069-015-1965-6.
- Vincent E. M., K. A. Emanuel, M. Lengaigne, J. Vialard, and G. Madec (2014), Influence of upper-ocean stratification interannual variability on tropical cyclones, *J. Adv. Model. Earth Syst.*, 6(3), 680–699, doi:10.1002/2014MS000327.
- Wada, A. (2015), Roles of the ocean on extremely rapid intensification and the maximum intensity of Typhoon Haiyan in 2013, *CAS/JSC WGN Res. Activities in Atm. And. Oceanic Modelling*, 45, 9.10–9.11.
- Wood, K. M., and E. A. Ritchie (2013), An updated climatology of tropical cyclone impacts on the southwestern United States, *Mon. Weather Rev.*, 141(12), 4322–4336, doi:10.1175/MWR-D-13-00078.1.
- Wu, C. C., W. T. Tu, I. F. Pun, I. I. Lin, and M. S. Peng (2016), Tropical cyclone-ocean interaction in Typhoon Megi (2010)—A synergy study based on ITOP observations and atmosphere-ocean coupled model simulations, *J. Geophys. Res. Atmos.*, 121(1), 153–167, doi:10.1002/2015JD024198.
- Yablonski, R. M., and I. Ginis (2008), Improving the ocean initialization of coupled hurricane-ocean models using feature-based data assimilation, *Mon. Weather Rev.*, 136(7), 2592–2607, doi:10.1175/2007MWR2166.1.
- Yeh, S. W., J. S. Kug, B. Dewitte, M. H. Kwon, B. P. Kirtman, and F. F. Jin (2009), El Niño in a changing climate, *Nature*, 461(7263), 511–514, doi:10.1038/nature08316.
- Yu, J. Y., Y. Zou, S. T. Kim, and T. Lee (2012), The changing impact of El Niño on US winter temperatures, *Geophys. Res. Lett.*, 39, L15702, doi:10.1029/2012GL052483.
- Zhang, Y., J. Chen, and Y. Du (2017), Role of barrier layer in the developing phase of “Category 6” super typhoon Haiyan, *Satell. Oceanogr. Meteorol.*, 2(1), doi:10.18063/SOM.2016.02.001.
- Zheng, Z. W., I. I. Lin, B. Wang, H. C. Huang, and C. H. Chen (2015), A long neglected damper in the El Niño – Typhoon relationship: A ‘Gaia-Like’ process, *Sci. Rep.*, 5(1), 11103, doi:10.1038/srep11103.